CHAPTER III
CHITOSAN NANOPARTICLES FOR HOUSE DUST MITE ALLERGEN DELIVERY: FROM A SIMPLE SINGLE STEP WATER-BASED CONJUGATION TO AN IMMUNOTHERAPY STUDY ON CELLULAR SAFETY AND PRECLINICAL IMPLEMENTATION

3.1 Abstract

The present work proposes a single step preparation of chitosan nanoparticles conjugated with biomolecules in water and demonstrates the potential use as allergen delivery system based on a house dust mite allergen (HDM) model. By simply mixing chitosan (CS) with hydroxybenzotriazole (HOBt), a water soluble chitosan can be easily obtained and this enables us an effective single step conjugation of phenylalanine and polyethylene glycol resulting in chitosan-phenylalanine-poly(ethylene glycol)methyl ether, CS-Phe-mPEG nanoparticles, in the range of 20-50 nm. The chitosan nanoparticles offer the electrostatic force and hydrophobic-hydrophobic van der Waals to immobilize and/or entrap the HDM as qualitatively and quantitatively analyses by zeta potential measurement, quartz crystal microbalance technique, and high performance liquid chromatography. An in vitro study of the HDM-entrapped CS-Phe-mPEG on both L929 Fibroblast-like cells, and HaCaTs keratinocyte cells clearly indicates the cell viability and non-toxicity. The in vitro preclinical implementation of HDM-entrapped CS-Phe-mPEG nanoparticles on peripheral blood mononuclear cells (PBMCs) from healthy- and HDM-allergic volunteers exhibits the immunogenicity (cell-mediated immune response). By the role of CS-Phe-PEG components, i.e. CS, Phe, and mPEG molecules, the HDM-entrapped CS-Phe-mPEG nanoparticles are capable of immune modulation and the survival of the PBMCs from HDM as evidence from the reducing of interferon-(IFN)-γ and interleukin-(IL)-10 secretions in PBMCs from HDM-allergic patients compared with normal controls.

Keywords: chitosan nanoparticles, water-based system, single step conjugation, immunogenicity, house dust mite allergen delivery system

3.2 Introduction

Chitosan is the second-most naturally abundant polysaccharide under the structure of β-(1-4)-2-acetamido-2-deoxy-β-D-glucose and β-(1-4)-2-amino-2-deoxy-β-D-glucose. Chitosan is accepted as a biomaterial with biodegradability (Zoldners *et al.*, 2005), biocompatibility (Molinaro *et al.*, 2002), and non-toxicity (Huo *et al.*, 2011). Structurally, chitosan is under strong inter- and intra- molecular hydrogen bonds, therefore, chitosan has no melting temperature and is insoluble in most solvents, water, but soluble in acids. Thus, functionalization of chitosan for potential biomaterials, in most cases, needs steps of modification to organo-soluble and/or water-soluble intermediates. The known cases are, for example, dimethylformamide (DMF) soluble phthaloylchitosan (Kurita *et al.*, 2001), and water soluble *N*-trimethylchitosan (TMC) (de Britto and Campana-Filho, 2004), *N,O*-carboxymethyl chitosan (CMC) (Aiba, 1989; Muzzarelli *et al.*, 1994), and *O*-succinyl chitosan (Kennedy *et al.*, 1996).

It is well known that polymeric nanoparticles can be easily formed if the polymer chains contain hydrophobic and hydrophilic groups to allow core-shell self assembly and there are many successful cases in the past such as polystyrene-*b*-poly(acrylic acid) (Zhang *et al.*, 2004), poly(t-butyl methacrylate)-*b*-poly(2-diethylaminoethyl methacrylate) (Mao *et al.*, 2005), and polystyrene-*b*-poly(2-vinyl pyridine)-*b*-poly(ethylene oxide) (Lei *et al.*, 2003). In similar, chitosan nanaparticles can be prepared by decorating with hydrophobic groups such as phthalimido group (Yoksan *et al.*, 2003) and linoleic acid group (Wang *et al.*, 2011), and hydrophilic groups such as poly(ethylene glycol) (Yoksan *et al.*, 2003) and poly(malic acid) (Wang *et al.*, 2011). The use of biomolecules, especially, peptides and/or amino acids e.g. phenylalanine (Phe) (Yoksan and Akashi, 2009), poly(amido amine) as hydrophobic groups is also a good strategy since not only the formation of nanoparticles but also the specific properties such as transfection efficiency, non-cytotoxicity, and transmembrane activity can be achieved.

Previously, chitosan was reported as a depot including adjuvant (Chew *et al.*, 2003; Taranejoo *et al.*, 2011) which is essential to increase the efficacy of allergen immunotherapy (Ameal *et al.*, 2005; Fernandez-Caldas *et al.*, 2006). Vila et al.

prepared chitosan nanoparticles by reprecipitating chitosan in acetic acid solution during mixing with tetanus toxoid. Their nanoparticles could cross nasal epithelia to increase the humoral immune response (Vila *et al.*, 2004). Slütter et al. reported that the crosslinked trimethylchitosan with ovalbumin via disulfide bond in water enhanced the immunogenicity (Slütter *et al.*, 2010). To our viewpoint, although chitosan is a potential biopolymer for biomedical applications, the organic solvents involved in the steps of chemical modifications always bring the questions of cell compatibility and viability. In fact, among the delivery systems, the allergen delivery concerns the most about cell compatibility and non toxicity since it already contains the allergen which is ready to stimulate cell irritation. Therefore, to our viewpoint, it is an ideal to derivatize chitosan in water with less steps in mild condition. In the past, we reported that hydroxybenzyltriazole (HOBt) enables chitosan to be soluble in water resulting in the possibility of the conjugating reaction in water (Fangkangwanwong *et al.*, 2006: Fangkangwanwong *et al.*, 2006) and this leads us to avoid the organic solvent contamination.

It comes to our question whether we can obtain the derivatization of chitosan in water for allergen delivery system. In this way, the cell compatibility as well as the synergistic effect of adjuvant and allergen delivery might be possible. The present work, therefore, proposes a simple preparation of chitosan nanoparticles by a single conjugation step in water. The conjugating hydrophobic and hydrophilic groups are considered based on the cell compatibility and therefore, the biomolecule, i.e. phenylalanine, and biocompatible polyethylene glycol are the choices to choose so that CS-Phe-mPEG is obtained. The work covers an in-vitro study to demonstrate the potential use by applying house dust mite allergen (HDM) extract (*Dermatophagoides pteronyssinus*) as a model and clarifying the cell compatibility in terms of cell viability and immunogenicity (cell-mediated immune responses), including allergen release profile. An in-vivo study based on the in vitro preclinical implementation on peripheral blood mononuclear cells (PBMCs) from HDM-allergic patients is extended to clarify how CS-Phe-mPEG performs the immune response by evaluating the interferon-(IFN)-γ and interleukin-(IL)-10 secretions in PBMCs from allergic patients.

3.3 Experimental Section

3.3.1 Materials

Chitosan (CS) (deacetylation degree (%DD) = 91, M_w ~ 15 kDa) was provided from Chitin Research Center Chulalongkorn University, Thailand. 1-Hydroxybenzotriazole monohydrate (HOBt·H_2O) and 1-ethyl-3-(3-dimethylaminopropyl-carbodiimide) hydrochloride (EDC·HCl) were purchased from Wako Pure Chemical Industries Co., Ltd., Japan. D,L-Phenylalanine (Phe) and succinic anhydride were obtained from Fluka Chemika, Switzerland. Poly(ethylene glycol) methyl ether (mPEG, M_n 5 kDa), fluorescein isothiocyanate (FITC), and trifluoroacetic acid (TFA) were bought from Sigma-Aldrich, Inc., USA. Allergen extract (*Dermatophagoides pteronyssinus*) with a concentration of ~ 260 µg/mL was purchased from ALK ABELLÓ, USA. Resazurin solution and PrestoBlue™ reagent were bought from Invitrogen, USA. Propidium iodide (PI) and 2′,7′-dichlofluorescein-diacetate (H_2DCF-DA) were purchased from Molecular probes, USA. Roswell Park Memorial Institute (RPMI) 31800-022 medium and Dulbecco's Modified Eagle Medium (DMEM) with 10% Fetal bovine serum (FBS), 1% penicillin/streptomycin were bought from Gibco, USA. Triton x-100, 4',6-diamidino-2-phenylindole (DAPI), trypsin, phosphate buffer saline (PBS), and ethylenediaminetetraacetic acid (EDTA) were purchased from Sigma-Aldrich, Inc., USA. Ficoll-Paque™ was bought from Lymphoprep, Norway. ELISA MAX™ standard set was purchased from Biolegend, USA. Methanol, dimethyl sulfoxide (DMSO), ethanol, and acetonitrile were purchased from RCI Labscan Co., Ltd., Thailand. All chemicals were used as received without further purification.

3.3.2 Preparation of Chitosan-Phenylalanine-Poly(ethylene glycol)methyl ether, CS-Phe-mPEG

CS (0.1 g, 0.61 mmol, 1.0 eq.) was vigorously stirred with HOBt (0.1 g, 0.73 mmol, 1.2 eq.) in deionized water (20 mL) at ambient temperature until clear solution. CS-HOBt solution was mixed with Phe (0.1 g, 0.61 mmol, 1.0 eq.), carboxyl terminated mPEG (mPEG-COOH) (0.9 g, 0.18 mmol, 0.3 eq.), and EDC (0.35 g, 1.82 mmol, 3 eq.) in 20 mL of deionized water (see appendix A for mPEG-

COOH synthesis). The reaction was carried out overnight at ambient temperature. The crude product obtained was dialyzed against water, lyophilized, washed with methanol, and dried under vacuum to obtain 1S-CS-Phe1.0-mPEG0.3. Similar reactions using mPEG-COOH for 0.3 equivalent mole (mol eq.) to CS but varying Phe to be 0.5, 1.5, 2.0, and 3.0 mol eq. to obtain 1S-CS-Phe0.5-mPEG0.3, 1S-CS-Phe1.5-mPEG0.3, 1S-CS-Phe2.0-mPEG0.3, and 1S-CS-Phe3.0-mPEG0.3, respectively were studied as well.

The two-step reaction was also carried out. In brief, CS (0.1 g, 0.61 mmol, 1.0 eq.) was stirred with HOBt (0.1 g, 0.73 mmol, 1.2 eq.) before adding Phe (0.1 g, 0.61 mmol, 1.0 eq.) and allowing the reaction at room temperature for 12 hours. The compound obtained was purified by dialysis and lyophilized to be CS-Phe1.0. The degree of Phe substitution was further confirmed by using ^{1}H-NMR. An amount of 0.3 mol eq. (0.9 g, 0.17 mmol) of mPEG-COOH was added into CS-Phe1.0 (0.1 g, 0.57 mmol) water solution containing HOBt (0.09 g, 0.68 mmol) and EDC (0.33 mg, 1.71 mmol) to obtain crude product. The crude was purified by dialysis and freeze-dried to obtain 2S-CS-Phe1.0-mPEG0.3. Similarly, 2S-CS-Phe3.0-mPEG0.3 was prepared by using CS-Phe3.0 and mPEG-COOH (0.3 mol eq. to CS-Phe3.0). In addition, the chitosan conjugated with mPEG-COOH, CS-mPEG0.3, was also synthesized by the same procedures but without the step of conjugation with Phe.

3.3.3 Structural Characterization by FT-IR and ^{1}H-NMR Spectroscopy

The chemical structures were analyzed by Fourier transform infrared (FT-IR) spectroscopy using a Bruker Equinox 55/S with 32 scans at resolution of 4 cm^{-1} in a frequency range of 4000-650 cm^{-1} using a deuterated triglycinesulfate detector (DTGD) with a specific detectivity, D*, of 1×10^{9} cm Hz ½ w^{-1}. The degrees of substitution (%DS) of Phe and mPEG-COOH were determined by using a Bruker Ultrashield 500 Plus proton nuclear magnetic resonance (^{1}H-NMR) (Figure B1).

3.3.4 Evaluation of Morphology, Size, and ζ -potential

The morphology and size of the samples in dry state were observed by an H-7650 Hitachi transmission electron microscope (TEM) at 100 kV.

The z-average diameter and ζ -potential of the samples in solution state were determined by a Malvern Zetasizer Nano Series (Malvern Instruments, Ltd.) with a detection angle of 173°, dynamic light scattering (DLS). In the case of ζ -potential, the laser doppler electrophoresis was applied based on the Henry's equation (Hunter, 1981).

3.3.5 Allergen Entrapment

The allergen entrapped was carried out in deionized (DI) water at pH 6. CS, CS-Phe1.0, 1S-CS-Phe1.0-mPEG0.3, and CS-mPEG0.3 (1 mg/mL) were mixed with HDM (16.25 µg/mL) and shaken vigorously for a minute at ambient temperature. The mixture was centrifuged and the supernatant was collected before determining the entrapment efficiency (EE), and the loading capacity (LC) of HDM-allergen according to Eqs (1), and (2), respectively. The HDM-entrapped particles obtained were lyophilized and kept in dried solid state at 4°C before conducting in vitro studies.

$$\%EE = \frac{(\text{initial allergen content} - \text{allergen content in supernatant})}{\text{initial allergen content}} \times 100 \quad (1)$$

$$\%LC = \frac{(\text{initial allergen content} - \text{allergen content in supernatant})}{\text{chitosan content}} \times 100 \quad (2)$$

3.3.6 Allergen Content Determination

The house dust mite allergen entrapped in each sample, i.e. CS, CS-Phe1.0, 1S-CS-Phe1.0-mPEG0.3, and CS-mPEG0.3, was determined by using a Shimadzu reversed-phase high performance liquid chromatography (HPLC), Japan equipped with a Vertisep^{TM} GES C_{18} HPLC column, 5 µm, 4.6 × 250 mm using the gradient mobile phase (mobile phase A: 0.1% TFA in water, mobile phase B: 0.085% TFA in acetonitrile) with a flow rate of 1.0 mL/min. The sampling injection

volume was 20 μL and the analysis was carried out at 30 °C. The sample was detected by using a Shimadzu UV-Vis detector at wavelength 290 nm. The retention time between 8.0-9.4 min was integrated to determine the HDM-allergen content.

The allergen immobilization efficiency was quantitatively analyzed by using an Affinix Q8 (Initium Co. Ltd, Tokyo) quartz crystal microbalance (QCM). The QCM gold probe was cleaned neatly and dried completely before dropping 1S-CS-Phe1.0-mPEG0.3 solution and HDM solution. The magnitude of frequency change (ΔF) was recorded and calculated by Eq. (3) to obtain the amount of HDM-allergen immobilized to 1S-CS-Phe1.0-mPEG0.3. The percent HDM immobilization was calculated by Eq. (4) (details in Scheme D1). The HDM immobilization under the different pH conditions (pH 3-10) were also studied with the same procedures.

$$\Delta F = \frac{-2 F_0^2}{A(\rho_q \mu_q)^{1/2}} \Delta M \qquad (3)$$

$$\text{Allergen immobilization efficiency (\%)} = \frac{\Delta M_2}{\Delta M_1} \times 100 \qquad (4)$$

Where ΔF is the frequency change of the crystal, F_0 is the fundamental frequency of the quartz, A is the area of the gold disk coated onto the quartz, ρ_q is the density of quartz, μ_q is the shear modulus of quartz, and ΔM_1 and ΔM_1 are the immobilized mass of 1S-CS-Phe1.0-mPEG0.3 solution and HDM solution, respectively, per surface area.

3.3.7 Cell Culture for In vitro Cytotoxicity

L929 Fibroblast-like cells, derived from mouse connective tissue (NCTC clone 929: CCL 1, American Type Culture Collection [ATCC]) were provided by the National Center for Genetic Engineering and Biotechnology (Thailand). They were grown in DMEM supplemented with 10% FBS and 1% penicillin/streptomycin in the humidified atmosphere of 5% CO_2 at 37°C. L929 cells

were removed from the culture flasks by enzymatic digestion (trypsin/EDTA) before centrifuging to collect the cells.

HaCaTs (human keratinocytes) were cultured in DMEM with 10% FBS and 1% penicillin/streptomycin and incubated in 5% CO_2 incubator at 37°C.

3.3.8 In Vitro Cytotoxicity

Cell viability

In vitro cytotoxicity studies for 1S-CS-Phe1.0-mPEG0.3, HDM-entrapped 1S-CS-Phe1.0-mPEG0.3, and the free HDM were evaluated by Alarmar blue and MTT assays (see appendix A for MTT assay). For Alarmar blue assay, L929 cells were seeded in the 96-well plate at a density of 1×10^4 cells/well. After the cells were incubated at 37 °C in the humidified 5% CO_2/ 95% air atmosphere for 24 h, 1S-CS-Phe1.0-mPEG0.3 with a series of the concentrations, i.e. 5, 2.5, 1.0, 0.5, 0.1 mg/mL, were added as well as 10% DMSO in DMEM with 5% FBS before incubating for 24 h. An amount of Resazurin solution (100 µL, 0.001% in DMEM) was further added to each well before incubating in the dark for 4 h. All wells were detected for fluorescence intensity at 530 nm/ 590 nm (excitation/emission) by a Perkin Elmer multimode plate reader VICTOR X4.

HaCaTs were seeded in 96-well plates at a density of 5×10^3 cells/well in 45 µL, and allowed incubating at 37°C and 5% CO_2 for 12 h. The cells were treated with 10 µg/mL allergen and the chitosans, i.e. CS, HDM-entrapped CS, CS-Phe1.0, HDM-entrapped CS-Phe1.0, CS-mPEG0.3, HDM-entrapped CS-mPEG0.3, 1S-CS-Phe1.0-mPEG0.3, and HDM-entrapped 1S-CS-Phe1.0-mPEG0.3, at a concentration 3 mg/mL in 45 µL and incubation time 24 h. Ten µL PrestoBlue™ reagent was added and cells were allowed incubating for 30 min before observing fluorescence using a Thermo Varioskan Flash (England) microplate reader at 560 nm and 590 nm. The mean fluorescence values corrected for a blank (i.e. media only) were calculated and used as the control. The relative cell viability was calculated as cell viability (%) (Eq. (5)).

$$\%\,\text{Cell viability} = \frac{OD_{sample}}{OD_{control}} \times 100 \qquad (5)$$

Cell morphology

HaCaTs were seeded in 24-well plates at a density of 5×10^4 cells/well and incubated at 37°C and 5% CO_2 for 12 h. The cells were treated with 10 µg/mL allergen and the chitosans, i.e. HDM-entrapped CS and HDM-entrapped 1S-CS-Phe1.0-mPEG0.3, at a concentration of 3 mg/mL and incubation time 24 h. Cell morphology was studied using a Nikon Eclipse TS 100 microscope (Japan).

ROS generation

HaCaTs were seeded in 96-black well plates at a density of 5×10^3 cells/well and incubated at 37°C and 5% CO_2 for 12 h. The cells were washed with phosphate buffer saline (PBS) before 0.1 µM of H_2DCF-DA was added at a volume of 100 µL/well. The cells were incubated for 30 min and washed again before treating with 10 µg/mL allergen and the chitosans, i.e. HDM-entrapped CS, HDM-entrapped CS-Phe1.0, HDM-entrapped CS-mPEG0.3, and HDM-entrapped 1S-CS-Phe1.0-mPEG0.3, at a concentration 3 mg/mL. Fluorescence was measured every 10 min for 1 h at 520 nm using a microplate reader.

Cell cycle assay

HaCaTs were seeded in 24-well plates at a density of 5×10^4 cells/ well and incubated at 37°C and 5% CO_2 for 12 h. The cells were then treated with 10 µg/mL allergen and the chitosans, i.e. HDM-entrapped CS and HDM-entrapped 1S-CS-Phe1.0-mPEG0.3, (3 mg/mL) for 48 h. The cells were collected by trypsinization, washed twice with PBS, and fixed with 70% (v/v) ethanol overnight. The cells were further treated with 50 µg/mL PI as an indicator for relative DNA content and 0.1% (v/v) Triton x-100, and allowed incubating for 30 min at 37°C in the dark. The cell cycle analysis, from G1/G2 to S and to M, was traced by using a Becton Dickenson flow cytometer (FACSCalibur, USA).

3.3.9 Cell Culture for Cytokine Analysis

An in vitro immune response in peripheral blood mononuclear cells (PBMCs) was studied. Blood samples from skin prick tests taken from 17 HDM-sensitized volunteers, and 10 HDM-unsensitized volunteers, were collected in

accordance with the approval of the Institutional Review Board of Faculty of Medicine, Chulalongkorn University, Bangkok, Thailand (IRB No. 506/56). The PBMCs were isolated from volunteers' blood using Ficoll-Paque™. The PBMCs were cultured in RPMI with 10% FBS and 1% Penicillin/Streptomycin in 37°C, 5% CO_2 incubator.

3.3.10 Cytokine Analysis for In Vitro Immune Response

The cells were seeded at a density of 10^6 cells/well in 24-well plates, and treated with 10 μg/mL allergen and the chitosans, i.e. HDM-entrapped CS, HDM-entrapped CS-Phe1.0, HDM-entrapped CS-mPEG0.3, and HDM-entrapped 1S-CS-Phe1.0-mPEG0.3, (3 mg/mL) for 5 d. The cell supernatants were collected and stored at −80°C. Sandwich ELISAs were used to detect secreted levels of IL-10 and IFN-γ, according to the manufacturer's instructions (ELISA MAX™ standard set).

3.3.11 Statistical Analysis

Cytokine content from ELISA was analyzed by the Mann Whitney U test. For cell viability of HaCaTs and ROS generation, ANOVA (Analysis of variance) was used, followed by the Tukey's multiple comparison test. Statistical analyses were considered significantly different at $p\text{-}value \leq 0.05$.

3.3.12 Localization of Chitosan Nanoparticles

HaCaTs (keratinocyte cells) were incubated at 37°C under 5% CO_2 for 12 h. After treating the cells with HDM-entrapped 1S-CS-Phe1.0-mPEG0.3 binding with FITC for 24 h, the nuclei were stained with DAPI. Then, the localization of the particles was determined by using a Nikon, Elipse Ti-U fluorescent microscope (Japan).

3.4 Results and Discussion

3.4.1 Synthesis and Characterization of CS-Phe-mPEG

As shown in Scheme 3.1, 1S-CS-Phe-mPEG and 2S-CS-Phe-mPEG were successfully prepared by conjugating Phe and mPEG-COOH to CS-HOBt (pH 5.1< pK_a of the amine of CS (Wang *et al.*, 2006)) with EDC as conjugating agent in aqueous system. The single step reaction (1S-CS-Phe-mPEG) and two-step reaction (2S-CS-Phe-mPEG) were applied and the structural analyses of the compounds obtained from both reactions were compared. The carboxylic acid groups of Phe and mPEG-COOH were reacted with amino- and/or hydroxyl- groups of CS using EDC to obtian O-acylurea intermediate. (Scheme B1). The intermediate enables the nucleophilic reaction between CS and Phe as well as mPEG-COOH resulting in amide and/or ester bonds.

Figure 3.1A shows the FT-IR spectra of 1S-CS-Phe1.0-mPEG0.3, and 2S-CS-Phe1.0-mPEG0.3. As compared to CS, the aromatic ring of Phe and aliphatic chain of mPEG can be confirmed at 750 cm^{-1} (CH of aromatic ring) and 2884 cm^{-1} (C-H of -CH_2-), respectively. The covalent linkages could be identified as ester at 1745 cm^{-1} (-COO-) and amide at 1650 cm^{-1} (amide I) and 1550 cm^{-1} (amide II) (Figure 3.1B). The curve fitting technique was applied to analyze quantitatively the changes of amide and ester bonds. Here, the significant increases of the integral ratios between the peaks of interest, i.e. amide (at 1550 cm^{-1}) and ester (at 1745 cm^{-1}), the decrease of amine (at 1595 cm^{-1}), and the internal standard, i.e. C-O-C of pyranose ring (at 895 cm^{-1}) were observed (Table B1).

^{1}H-NMR spectra (Figures 3.2b and c) show the new signals at 7.36-7.24 ppm for C_6H_5 (H-c) of Phe, at 2.75-2.25 ppm for $COCH_2CH_2CO$ (H-d), and at 3.28 ppm for CH_3 (H-f) of mPEG. The degree of substitution (%DS) of Phe and mPEG were determined (Table B2, and Figure B2)and surprisingly, it was found that the %DS of Phe and mPEG of the single step and of the two-step reactions were nearly equal, for example in the case of using 1.0 and 0.3 mol eq. of Phe and mPEG,. By varying the mol eq. of Phe from 0.5 to 3.0 in the single step reaction, the %DS of Phe and mPEG were decreased from ~16 to ~6, and from ~14 to ~5, respectively. The optimal condition was found to be 16 % DS of Phe and 14 % DS of mPEG when the feed ratios were 1 and 0.3 mol eq., respectively. The result also indicated that Phe and mPEG might hinder the reaction when the amount of those reactants was above a certain level.

Scheme 3.1 Preparation of CS-Phe and CS-Phe-mPEG by a single step (1S) and two-step reactions (2S).

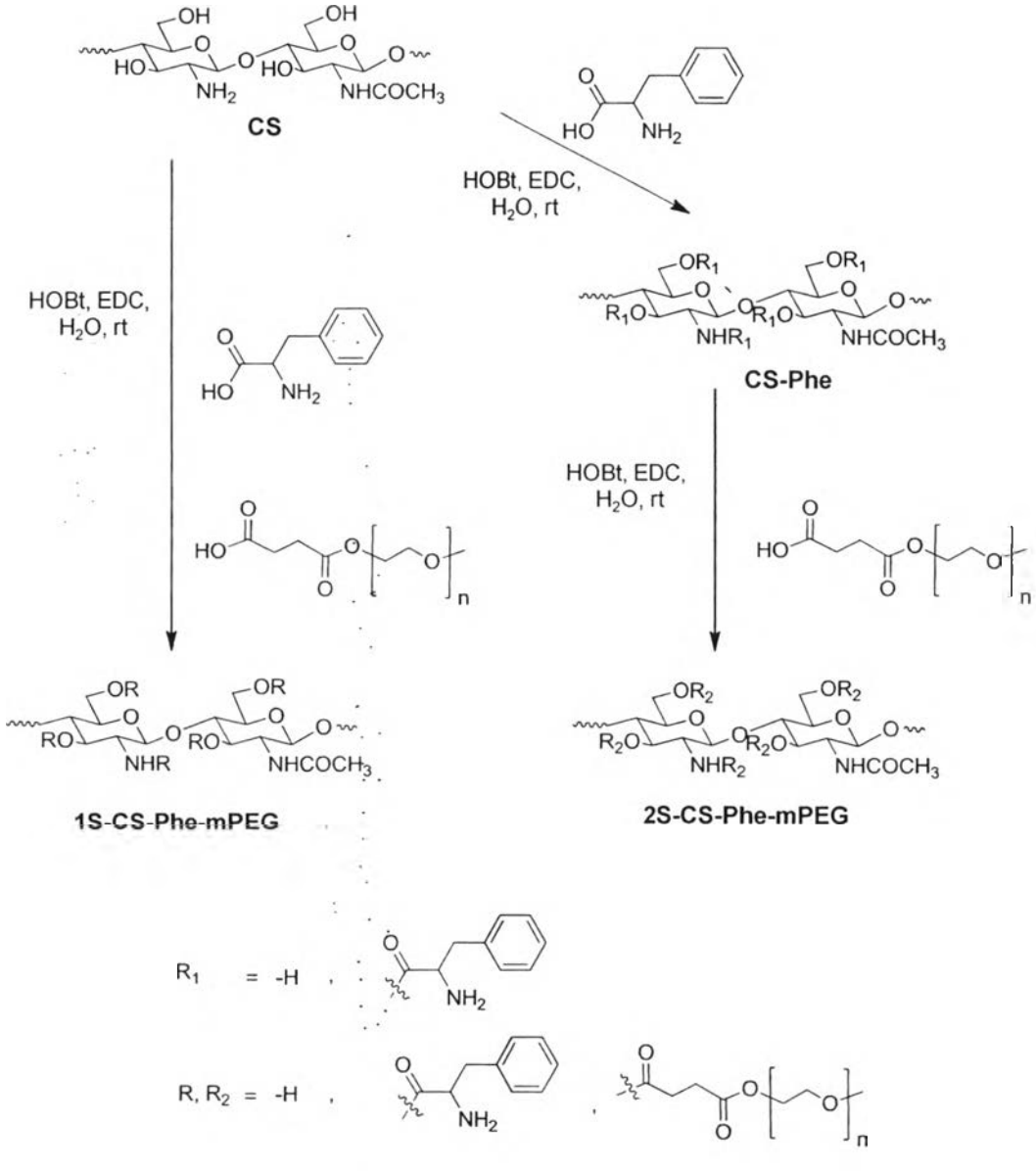

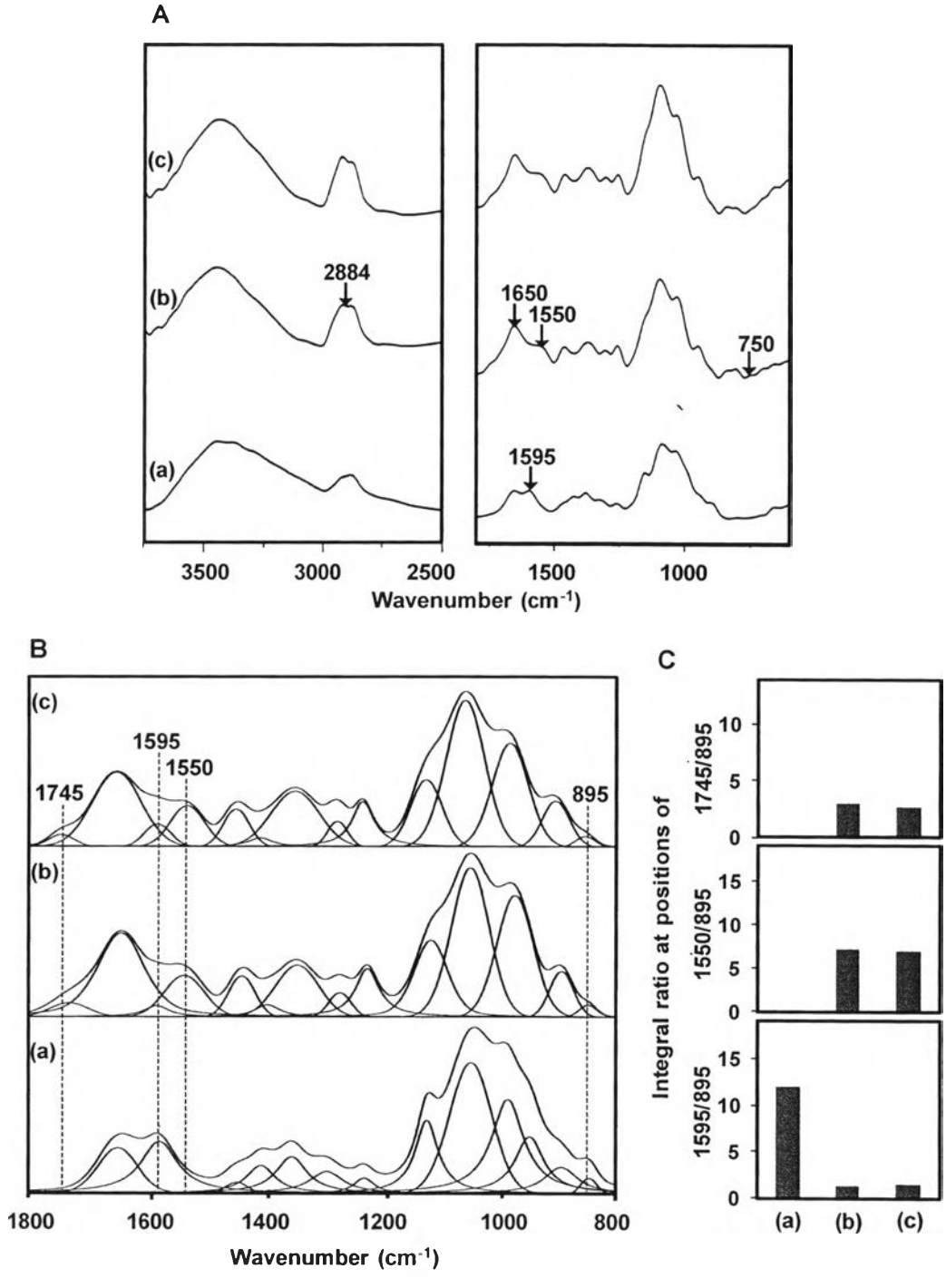

Figure 3.1 (A) FT-IR spectra, (B) region of FT-IR curve fitting, and (C) FT-IR curve fitting of (a) CS, (b) 1S-CS-Phe1.0-mPEG0.3, and (c) 2S-CS-Phe1.0-mPEG0.3.

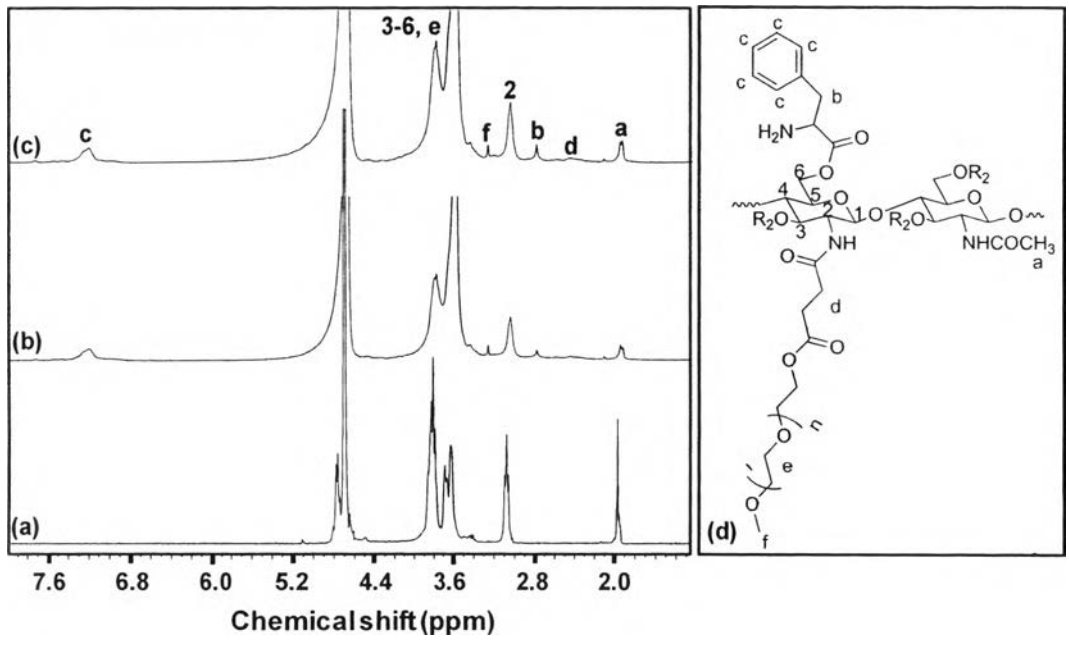

Figure 3.2 ^{1}H NMR spectra of (a) CS, (b) 1S-CS-Phe1.0-mPEG0.3, and (c) 2S-CS-Phe1.0-mPEG0.3 (in 2% CD_3COOD/D_2O), and (d) chemical structure of CS-Phe1.0-mPEG0.3 indicating the position of the protons.

3.4.2 Evaluation of Morphology, Size and ζ -potential

TEM was applied to determine the average diameter size and the morphology of CS, 1S-CS-Phe0.5-mPEG0.3, and 2S-CS-Phe1.0-mPEG0.3 in dry state (Figure 3.3). After CS was conjugated with Phe and mPEG (Figure 3.3b - c), 1S-CS-Phe0.5-mPEG0.3 and 2S-CS-Phe1.0-mPEG0.3 show the well separated particles with the sizes in the range of 20-50 nm and 30-50 nm, respectively, as compared to the aggregated CS (Figure 3.3a). It is important to note that for the high %DS of Phe (15 – 17 %) and mPEG (11 – 14 %) derivatives, i.e.1S-CS-Phe1.0-mPEG0.3, and 2S-CS-Phe1.0-mPEG0.3, the particles were in well separated nanoparticles whereas for the low %DS of Phe (12 – 6 %) and mPEG (9 – 5 %), i.e. 1S-CS-Phe1.5-mPEG0.3, 1S-CS-Phe2.0-mPEG0.3, and 1S-CS-Phe3.0-mPEG0.3 (Figure C1), the particles were randomly aggregated. These results indicate that the introduction of Phe and mPEG as hydrophobic and hydrophilic molecules induces the the nanoparticle formation whereas the optimal substitution brings the individual nanoparticles with stabiltiy.

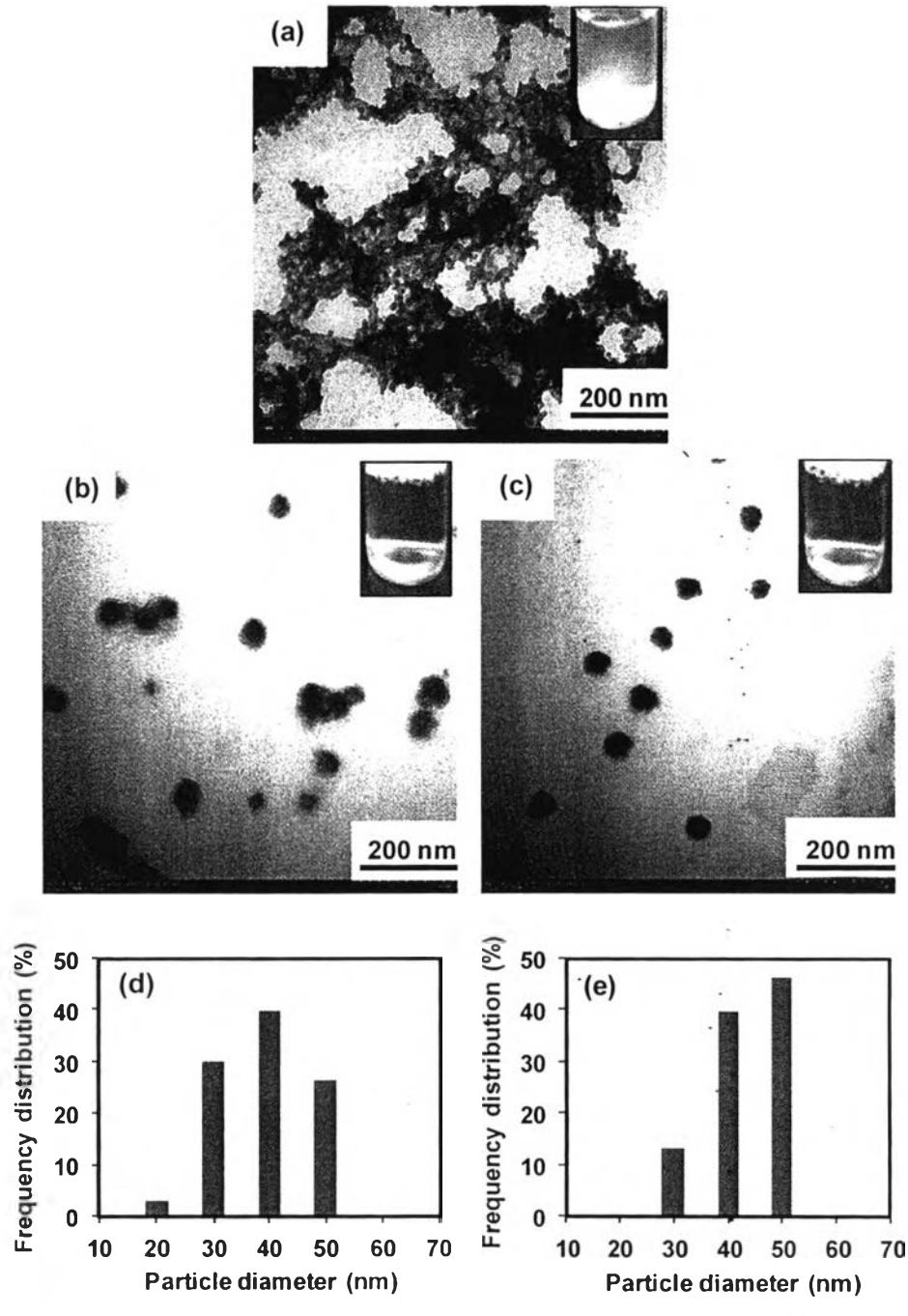

Figure 3.3 TEM micrographs, colloidal appearances, and frequency distribution of (a) CS, (b, d) 1S-CS-Phe1.0-mPEG0.3, (c, e) 2S-CS-Phe1.0-mPEG0.3.

In general, chitosan is water insoluble as shown as white precipitates in water (Figure 3.3a). After modification, 1S-CS-Phe1.0-mPEG0.3 and 2S-CS-Phe1.0-mPEG0.3 give colloidal solution (Figure 3.3b - c). It was found that the

colloidal state was maintained for more than 24 hours. At that time, mPEG-COOH might form the hydrogen bonds with water whereas the Phe might form the hydrophobic van der Waals interaction as the core of the nanoparticles. In order to confirm this, the dynamic changes of the particle size was observed by DLS under the variation of the dielectric constant (ε_m) of solvents. Here, the binary mixtures of protic solvents (water/ 2-propanol) and various types of protic solvents (water, ethanol, methanol, 2-propanol) were applied. It was found that the size of 1S-CS-Phe1.0-mPEG0.3 increased from ~200 nm to 2700 nm when the ε_m and solvent polarity decreased (Figure C3, C4). The decrease in polarity of aqueous solution leads to the obstructive effect of the hydrogen bond formation between the nanoparticles and water This resulted in a sudden aggregation of the samples.

It should be noted that the size, shape, frequency distribution of size (Figure 3.3d - e) of 1S-CS-Phe1.0-mPEG0.3 and 2S-CS-Phe1.0-mPEG0.3 preparing from single step and two-step reactions are similar. This implies that the conjugation of hydrophobic and hydrophilic groups are efficient and no obstructive effect to each other. It is also clear that the size was controlled by the % DS of Phe and mPEG rather than the step of the reactions. In the following session, 1S-CS-Phe1.0-mPEG0.3 which is considered as the optimal sample, is applied for further studies.

3.4.3 Evaluation of Allergen Entrapment

As allergen entrapment was carried out by mixing 1S-CS-Phe1.0-mPEG0.3 with crude allergen, it comes to the question how the physisorption was effective and stable. So, the ζ -potentials which represent the net charge on the surface of the particles were traced. Here, the ζ -potentials of HDM, 1S-CS-Phe1.0-mPEG0.3, and HDM-entrapped 1S-CS-Phe1.0-mPEG0.3 were observed at pH ~3 - 10. All compounds exhibit amphoteric ζ -potential curves with the different isoelectricity (pI) values where the ζ -potential value was zero (Figure 3.4). For example, the pIs of HDM and 1S-CS-Phe1.0-mPEG0.3 are 5 and 7.5, respectively, whereas that of HDM-entrapped 1S-CS-Phe1.0-mPEG0.3 is 6.5. It should be noted that after allergen-entrapping, the pI value of 1S-CS-Phe1.0-mPEG0.3 is shifted

down to be similar level to that of allergen. This implies the allergen entrapment is directly related to the electrostatic attraction.

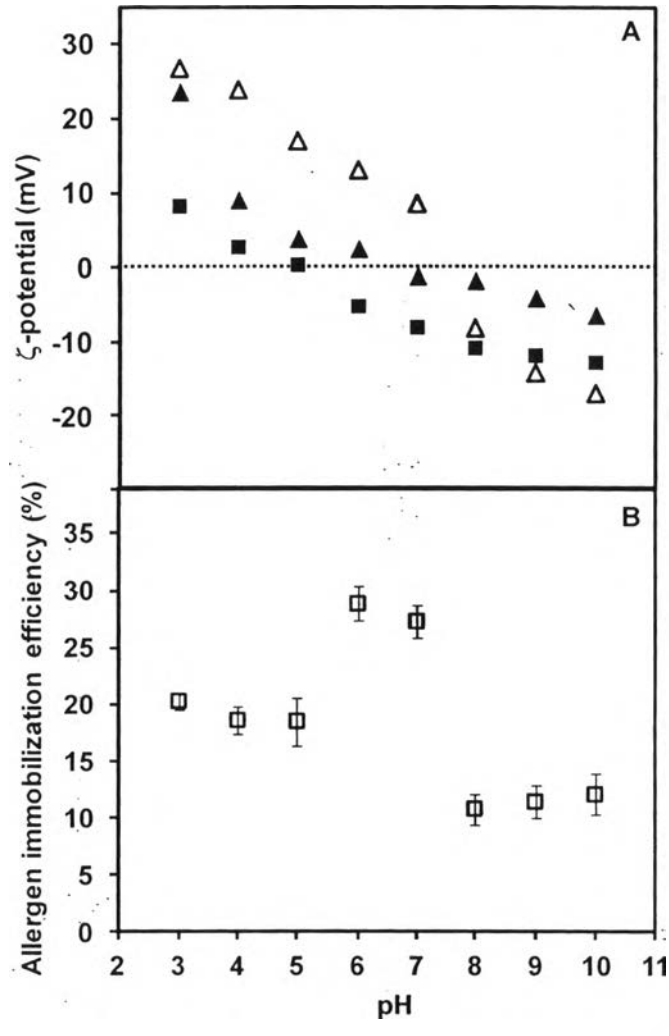

Figure 3.4 (A) ζ -potentials of (■) HDM, (Δ) 1S-CS-Phe1.0-mPEG0.3, and (▲) HDM-entrapped 1S-CS-Phe1.0-mPEG0.3 (concentration 1 mg/mL in HCl_{aq}/ $NaOH_{aq}$ solution), and (B) HDM immobilized content (%) of HDM-entrapped 1S-CS-Phe1.0-mPEG0.3 measured by QCM. Results are the means ± SD (n=3).

The QCM is a good technique to confirm the HDM immobilization efficiency based on the frequency changes as a consequence of the weight changes. Here, the HDM-immobilized 1S-CS-Phe1.0-mPEG0.3 evaluated by QCM in various pHs. The pH range at 6 - 7 gives percent immobilization efficiency as high as 26 –

30 % (Figure 3.4B). It is important to note that this pH range is where the individual HDM and 1S-CS-Phe1.0-mPEG0.3 show the opposite ζ potential value (Figure 3.4A). In fact, our result is relevant to the report by Yu et al. (Yu *et al.*, 2006) which showed the interaction between chitosan and ovalbumin was under electrostatic attraction. In their case, the sample was prepared in aqueous solution at pH 4.9 - 7.9 where chitosan and ovalbumin showed the opposite charges. In our case, by simply mixing HDM and 1S-CS-Phe1.0-mPEG0.3 at room temperature, not only the allergen entrapment and/or immobilization but also the nanoparticles in the sizes of 80 – 200 nm are quantitatively obtained (Figure 3.11a).

It should be also noted that at pH 3 - pH 5 and pH 8 - pH 10, even 1S-CS-Phe1.0-mPEG0.3 and HDM are not the opposite electrostatic charge to each other (Figure 3.4A), the immobilization content can also be observed (Figure 3.4B). This indicated other possible weak interactions formed between 1S-CS-Phe1.0-mPEG0.3 and allergen.

Hereinafter, 1S-CS-Phe1.0-mPEG0.3, CS-Phe1.0, and CS-mPEG0.3 are abbreviated as CS-Phe-mPEG, CS-Phe, and CS-mPEG, respectively. The percentage of entrapment efficiency (%EE) and loading capacity (%LC) of allergen are further evaluated by HPLC. Table 3.1 shows CS-Phe with the highest %EE and %LC. This implies that Phe plays an important role on not only electrostatic attraction but also the hydrophobic-hydrophobic secondary force (Kono *et al.*, 2004; Yoksan and Akashi, 2009). In other words, the hydrophobic-hydrophobic van der Waals between Phe moiety and protein allergen might also lead to the allergen entrapment.

Table 3.1 shows that the %EE of HDM-entrapped CS-Phe, CS-mPEG, and CS-Phe-mPEG are in the range of 20-30 %. This result is relevant to the report of Aktaş et al (Aktaş *et al.*, 2005). In their case, the %EEs of the bioactive molecules such as ovalbumin (Bal *et al.*, 2012), exotoxin A (subunit antigen) (Taranejoo *et al.*, 2011), and DNA (Yoksan and Akashi, 2009) were above ~30%. In fact the factors related to the entrapment efficiency are not clear. In our case, it is expected that the electrostatic force and hydrophobic-hydrophobic van der Waals might be the main factor.

Table 3.1 Entrapment efficiency (%EE), loading capacity (%LC), and diameter size (initial loaded allergen 16.25 μg/mL, and weight of chitosan derivatives 1 mg/mL)

Samples	%EE	%LC	Size (d-nm)	
			Before allergen entrapment	After allergen entrapment
CS	10.8± 2.8	0.2± 0.04	1950.0 ± 180.0	N/A
CS-Phe	30.7± 8.5	0.5± 0.14	774.9 ± 62.4	889.7 ± 84.6
CS-mPEG	21.1± 4.7	0.3± 0.08	187.4 ± 13.8	262.4 ± 38.7
CS-Phe-mPEG	21.6± 4.5	0.4± 0.07	287.2 ± 86.8	391.1 ± 41.6

It is important to point out the factors related to the retardance of the allergen entrapment. For example, it is clear that the %EEs of HDM-entrapped CS-mPEG and CS-Phe-mPEG are slightly lower than that of HDM-entrapped CS-Phe (Table 3.1). This indicates the possibility that mPEG chain obstructs the electrostatic attraction between CS and allergen. However, the hydrophilic mPEG in CS-Phe-mPEG plays the role of nanoparticle forming due to hydrophilic-hydrophobic self assembly resulting in obtaining smaller size compared to the size of CS-Phe (Table 3.1).

Additionally, the sizes of CS-Phe-mPEG, CS-Phe, and CS-mPEG, before and after HDM entrapment were investigated by DLS (Table 3.1). After HDM entrapment, the particle sizes are increased which reflects how the allergen entrapment in the nanoparticles was successful.

3.4.4 Cytotoxicity

Alarmar blue and MTT assay were applied for the studies of cytotoxicity. Here, L929 cells were chosen as a model study to clarify the biocompatibility (Figures 3.5A and 3.5B). After incubating for 24 h at 37 °C in the presences of the samples, i.e. CS-Phe-mPEG, HDM, and HDM-entrapped CS-Phe-mPEG, with the concentrations of 0.1, 0.5, 1.0, 2.5 mg/mL, the % cell viability for CS-Phe-mPEG, and HDM-entrapped CS-Phe-mPEG are above 80%. This indicates that CS-Phe-mPEG has no toxicity to the fibroblast cells. In the case of HDM, IC50 is shown at 5 mg/mL. However, even at that concentration, no IC50 found for CS-Phe-mPEG and HDM-entrapped CS-Phe-mPEG. This result implies that CS-Phe-mPEG decreases the cytotoxicity of allergen to the cell. The fact behind this might

related to the shielding of mPEG chains on the cell which prevented the attachment of the allergen to the cells as reported by Mao (Mao *et al.*, 2005) and Casettari (Casettari *et al.*, 2010).

Additionally, in order to clarify whether our system practical for non-parenteral routes or not, HaCaTs are selected as another model due to their ease of culture, fast growth, and their antigen presenting cell function (Giudice and Campbell, 2006).

After HaCaTs were treated with HDM and HDM-entrapped chitosans, the results show the similar cell morphology for all cases (Figure 3.6A). In addition, no significant differences of cell viability were observed (Figure 3.6B). The results suggest that CS and its derivatives do not show the effect on cellular structure, implying the biocompatibility for human keratinocytes. It is important to note that the cell viability is significantly increased in all treatments of HDM and HDM-entrapped chitosans when comparing with the control. This indicates the release of mitochondrial dehydrogenase and the consequence of converting resazurin to a fluorescence product as reported by Zhang et al (Zhang *et al.*, 2004).

The production of ROS implies the induction of cellular inflammation (Mittal *et al.*, 2014). Here, an ROS generation assay was used to evaluate HaCaT cell stress after treating with HDM and HDM-entrapped chitosans. Figure 3.7 shows that only HDM induces ROS generation whereas other HDM-entrapped chitosans including the control maintain ROS generation. In addition, for HDM, when the treatment time increased, the ROS generation increases significantly. This implies chitosan derivatives play an important role in controlling ROS production. In other words, our system shows potential decrease of cellular inflammation.

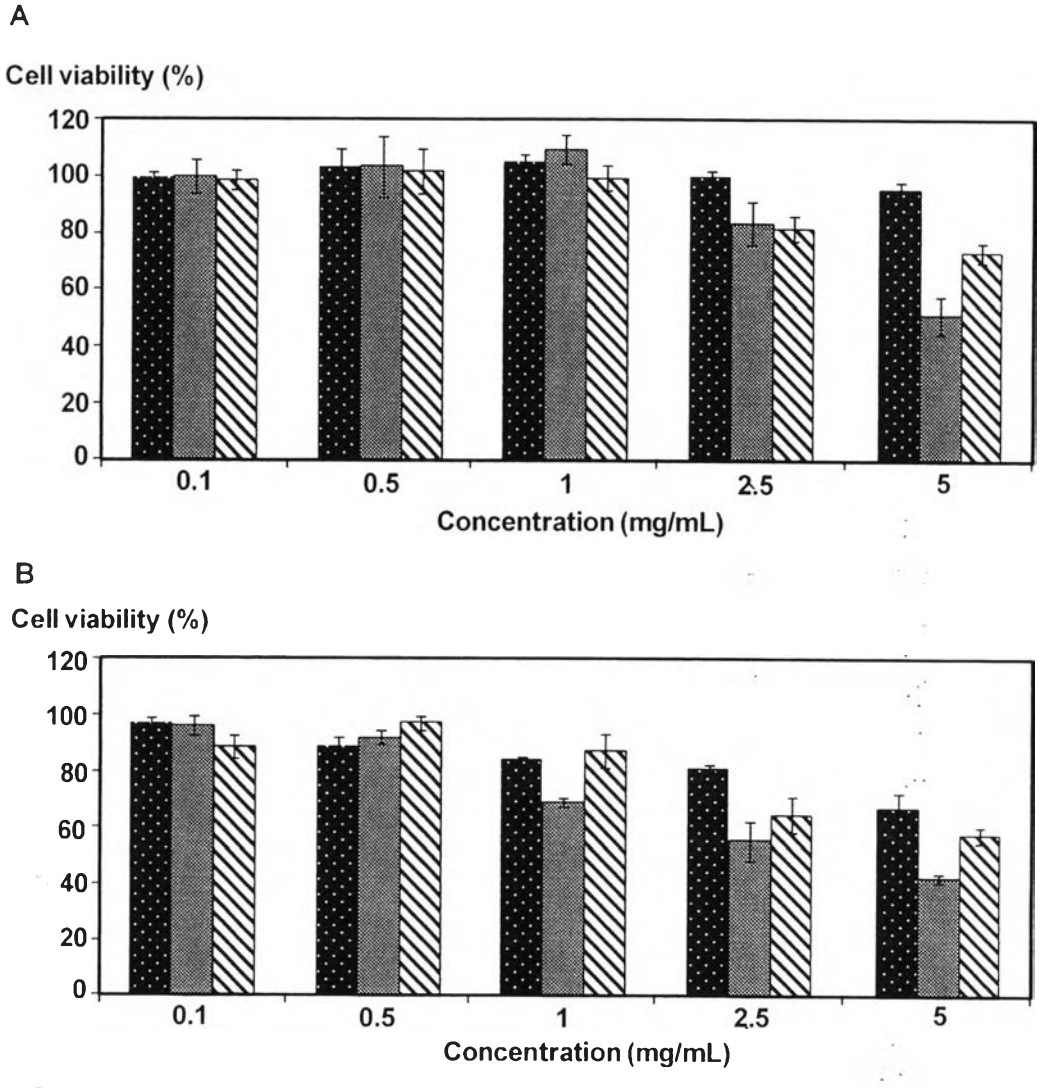

Figure 3.5 Cell viability of L929 cells determined by (A) Alarmar blue and (B) MTT assay in various concentration of ( ) CS-Phe-mPEG, ( ) HDM, and ( ) HDM- entrapped CS-Phe-mPEG.

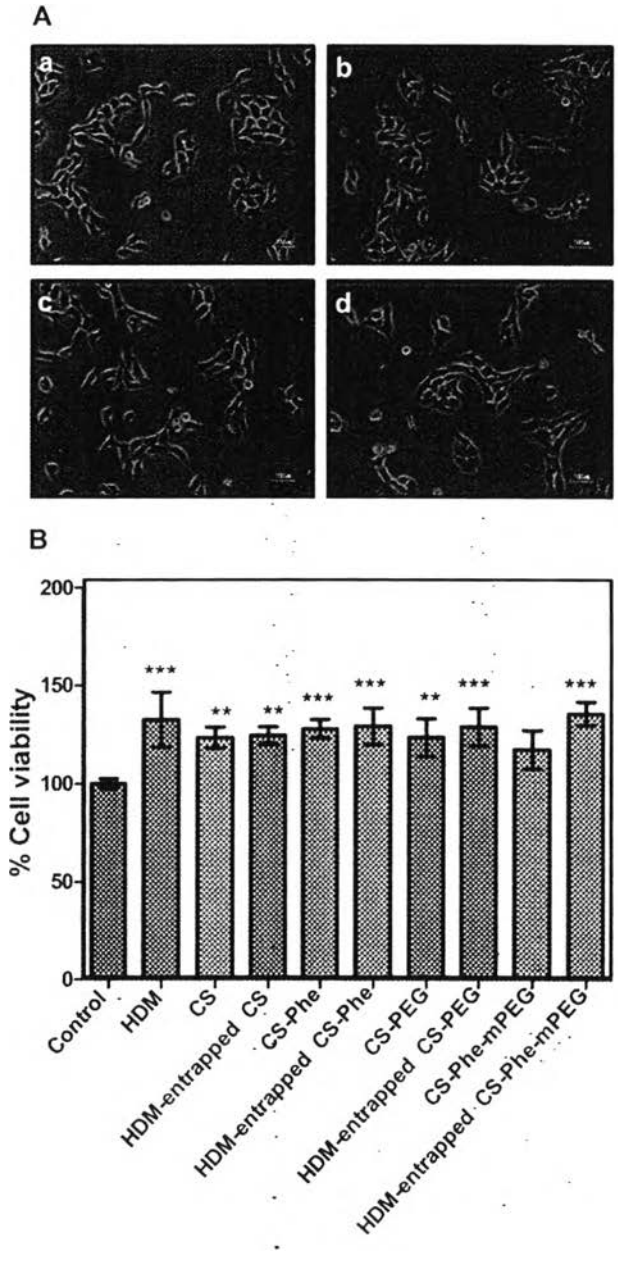

Figure 3.6 (A) Cell morphology of HaCaTs treated with (a) control, (b) HDM, (c) HDM-entrapped CS, and (d) HDM-entrapped CS-Phe-mPEG visualized by phase contrast microscopy and (B) Cell viability of HaCaTs treated with control, HDM, CS, HDM-entrapped CS, CS-Phe, HDM-entrapped CS-Phe, CS-mPEG, HDM-entrapped CS-mPEG, CS-Phe-mPEG, and HDM-entrapped CS-Phe-mPEG for 24 h.

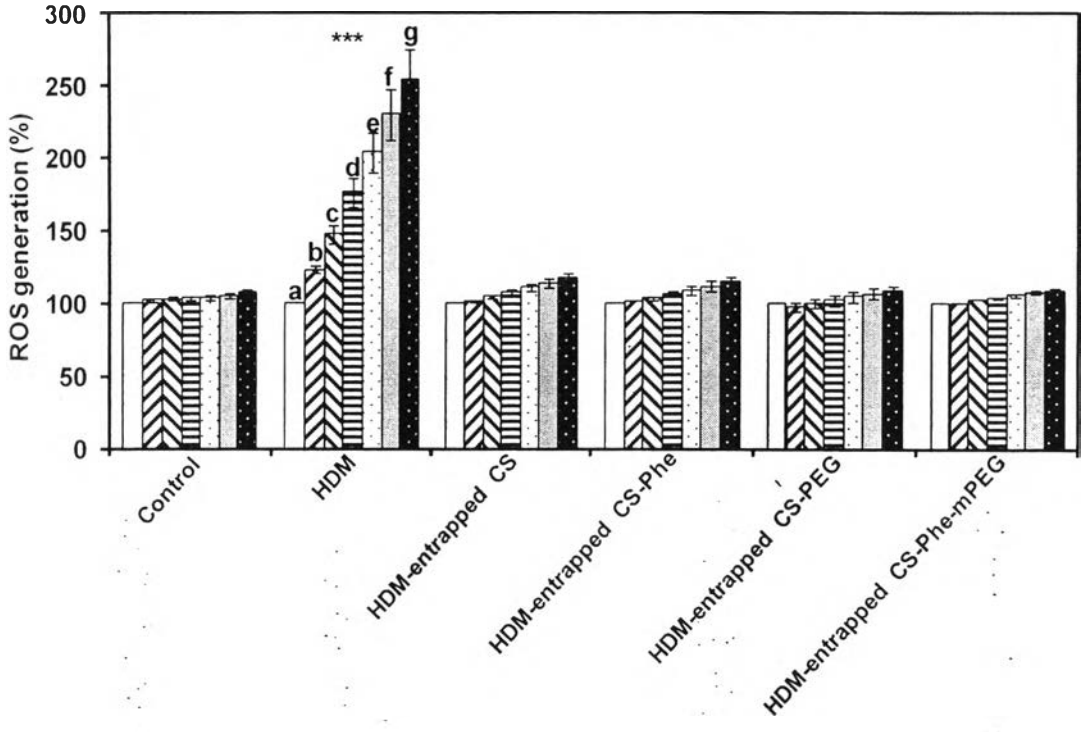

Figure 3.7 ROS generation from HaCaTs after treating with control, HDM, HDM-entrapped CS, HDM-entrapped CS-Phe, HDM-entrapped CS-mPEG, and HDM-entrapped CS-Phe-mPEG for a: 0 min, b: 10 min, c: 20 min, d: 30 min, e: 40 min, f: 50 min, and g: 60 min.

Figure 3.8 shows the cell proliferation/division of HaCaTs. Figure 8A indicates that HaCaTs in the control distributes the most in G1/G2 phase (~65%) and the least in G2/M phase (~14%). When HDM was added in the system, it is clear that G2/M phase was reduced significantly to be as low as 0.3%. In fact, apoptotic cells are also observed as seen from the relative DNA content intensity at ~100. This suggests how HDM disturbs the cell proliferation. In the cases of the cells treated with HDM-entrapped CS and HDM-entrapped CS-Phe-mPEG, the percentages of G1/G2 phase, S phase, and G2/M phase are similar to that of the control. In addition, no apoptotic cells observed. This indicates that when HDM was entrapped in chitosans, the disturbance of HaCaT proliferation was suppressed.

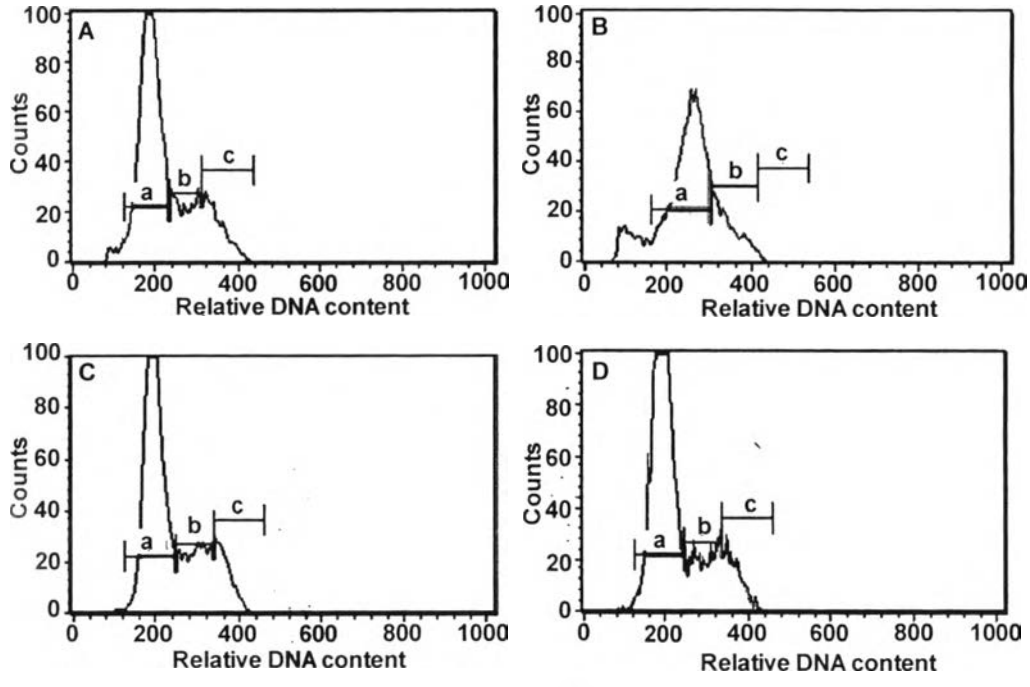

Figure 3.8 Cell cycle analysis of HaCaTs treated with (A) Control, (B) HDM, (C) HDM-entrapped CS, and (D) HDM-entrapped CS-Phe-mPEG. The cell cycle phases are shown as (a) G0/G1 phase, (b) S phase, and (c) G2/M phase.

3.4.5 Cell-mediated Immune Response to Allergen Immunotherapy in PBMC

In order to determine the function of HDM-entrapped CS-Phe-mPEG in stimulating cell-mediated immune system in term of T cell's cytokine response, the HDM and HDM-entrapped chitosans were incubated with PBMCs.

The productions of IFN-γ and IL-10 (Figure 3.9) in the cases of control for allergic- and healthy- subjects (a, b), do not exhibit any increases. In other words, there is no cytokine production. In fact, when the cells were incubated with HDM (c, d), the cell viability in PBMCs decreases. The results confirm how the allergen treatment causes cellular toxicity in PBMCs. This was further confirmed by observing the PBMC viability (Figure E2).

For HDM-entrapped chitosans, it is clear that the cytokine contents are increased. The significant changes can be seen in the case of HDM-entrapped CS-Phe-mPEG. At that time, the healthy-subjects show the IFN-γ and IL-10 as high

as ~0.38 ng/mL and 0.32 whereas the allergic subjects show those for ~0.3 ng/mL and 0.52 ng/mL respectively.

Here, the discussions on the role of CS-Phe-mPEG as nanoparticle for immune response in terms of the induction T helper 1 (Th1) (represented by IFN-γ) and regulatory T cell (Treg) (represented by IL-10) are as follows. The IFN-γ secretions (Figure 3.9A) from the allergic-subjects treated with control (b), HDM (d), HDM-entrapped CS (f), HDM-entrapped CS-Phe (h), and HDM-entrapped CS-mPEG (j) are similar level. The result reveals that the modifications with either Phe or PEG including CS do not induce Th 1 response. Whereas, the cells treated with HDM-entrapped CS-Phe-PEG secretes the highest levels of IFN-γ. This might come from the synergistic effect induced by the component of CS-Phe-PEG, i.e. CS, Phe, and mPEG molecules to effectively induce IFN-γ production in allergic-cells. Additionally, the stability and the size at nanometer level of CS-Phe-PEG might also function in uptaking the cells via endocytosis (Couvreur and Puisieux, 1993) resulting in the induction of cytokine release.

The synergistic effect and the stable nanoparticle are emphasized when it comes to the case of healthy subjects as seen from the highest secretion of IFN-γ. Comparing IFN-γ levels between the healthy and allergic subjects, the IFN-γ levels of HDM-entrapped CS-Phe, HDM-entrapped CS-PEG, and HDM-entrapped CS-Phe-PEG (~0.3 ng/mL), from allergic subjects, are lower than those of the healthy subjects (~0.38 ng/mL for HDM-entrapped CS-Phe-mPEG in the healthy cells). This result indicates that HDM-entrapped CS-Phe, HDM-entrapped CS-mPEG, and HDM-entrapped CS-Phe-PEG could modulate Th1 activity in allergic cells after 5 d. It is important to note that the results are relevant with the reports by Ghaemmaghaml et al. (Ghaemmaghami *et al.*, 2001). In their case, the IFN-γ secretion was suppressed in the human T cells stimulating with the Der p 1 allergen from HDM.

Considering IL-10 secretion (Figures 3.9B), the result shows that cells treated with HDM-entrapped chitosans secreted the higher IL-10 than the cells in the control condition. Especially, the IL-10 secretion of cells treated with HDM-entrapped CS-Phe-PEG (k, l) was higher than those of HDM-entrapped CS (e, f), HDM-entrapped CS-Phe (g, h), and HDM-entrapped CS-mPEG (i, j) for both

allergic and healthy subjects. This also confirms the role of the synergistic effects of CS, Phe, and PEG composition together with the stable nanoparticles. It is clear that IL-10 belonging to the allergic- (~0.32 ng/mL) is lower than the one belonging to the healthy-subjects (~0.52 ng/mL).

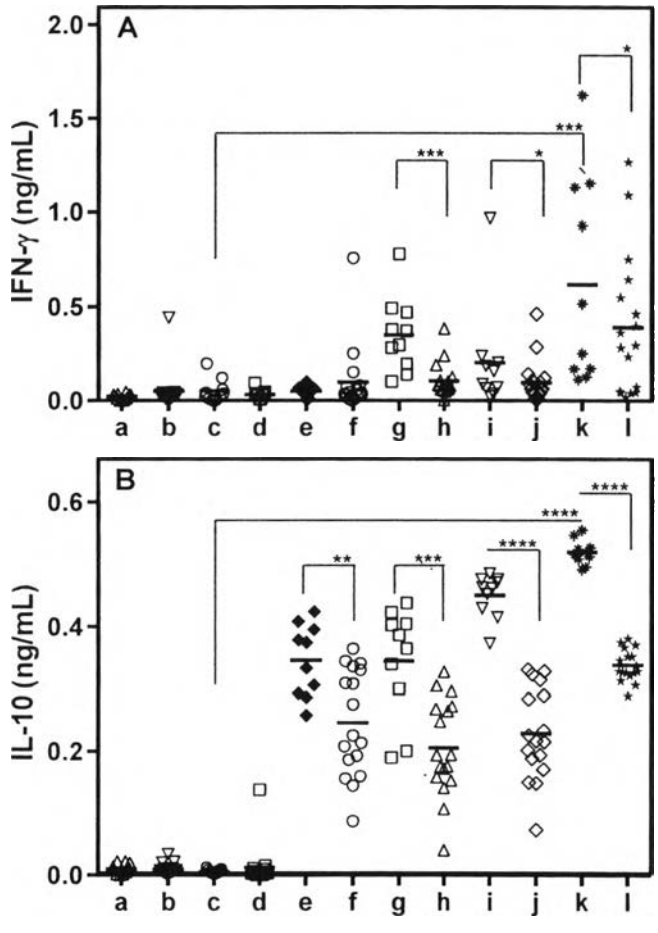

Figure 3.9 (A) IFN-γ and (B) IL-10 productions from PBMCs incubated with control (a-b), HDM (c-d), HDM-entrapped CS (e-f), HDM-entrapped CS-Phe (g-h), HDM-entrapped CS-mPEG (i-j), and HDM-entrapped CS-Phe-mPEG (k-l). PBMCs isolated from the normal (a, c, e, g, i, and k) and the allergic patients (b, d, f, h, j, and l).

Our results agree with that reported by Han et al. (Han *et al.*, 2010). In their case, they showed that IL-10-secreting regulatory T cells decreased in the blood

of rhinitis patients after D. *pteronyssinus*-allergen immunotherapy. However, Cosmi et al. (Cosmi *et al.*, 2006) found that IL-10 secretion was increased after stimulation of sensitized cells with the Der p 1 allergen of HDM. The decrease of IL-10 secretion by PBMCs might represent the systemic (blood circulation) IL-10 production. It is possible that IL-10 production following alternative routes of HDM-entrapped chitosans administration, such as subcutaneous, nasal, and oral, might be varied due to the specific responses of each cell type.

3.4.6 Localization of Particles to Cells

Figure 3.10 shows the green dots of FITC tagged with HDM-entrapped CS-Phe-mPEG at the surrounding of nuclei which is the region of cytoplasm. This result indicates the successful uptake of HDM-entrapped CS-Phe-mPEG into HaCaTs. Slutter et al.also reported that the ovalbumin-loaded N-trimethyl chitosan coated poly(lactic-co-glycolic acid) particle with the size less than 500 nm could uptake to dendritric cells (Slütter *et al.*, 2010).

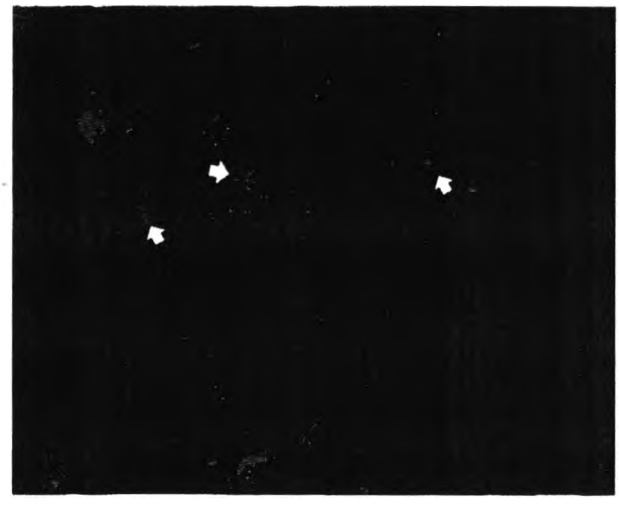

Figure 3.10 Fluorescent image of FITC-HDM-entrapped CS-Phe-mPEG (green dots) incubated with HaCaTs for 24 h. The blue region represents the nuclei stained with DPI.

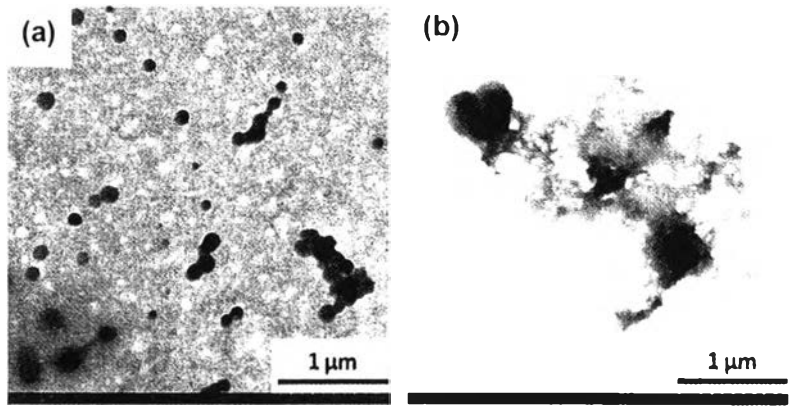

Figure 3.11 TEM micrographs of HDM-entrapped CS-Phe-mPEG (a) before HDM release, and (b) after HDM release.

In order to observe the potential of chitosan nanoparticles in allergen delivery system, an *in vitro* release profile of allergen from HDM-entrapped CS-Phe-mPEG was investigated at 37 °C in various buffers, i.e. citric acid/trisodium citate buffer (pH 5.2), phosphate buffer saline (PBS, pH 7.4), and tris buffer (pH 8) (Figure F1) to simulate the conditions of nasal (pH 5.5-6.5 and 7.2-8.3 in rhinitis (England *et al.*, 1999)) and plasma (pH 7.38-7.42 (Atherton, 2003)) treatments. In this work, it was found that a burst release of HDM-entrapped CS-Phe-mPEG occurred within the period of 10-12 h in tris buffer and within 62-65 h for citric buffer. In the case of alkaline pH (in tris buffer), as chitosan and its derivatives are deprotonated, this might lead to a significant allergen diffusion rate as compared to the case of acidic pH (citric buffer). The allergen release rate in PBS buffer was higher than in citric buffer and lower than in tris buffer. The result suggests the electrostatic effect as the key for the release profile. The total concentration of the released allergen was 50-55 % in both tris and PBS buffers, and 40 - 45 % in citric buffer. After *in vitro* release, it is clear that the original spherical shape of the HDM-entrapped CS-Phe-mPEG was distorted and became bigger (Figure 3.11b). This implies the swelling behavior after the allergen releasing in the buffers.

3.5 Conclusions

Chitosan nanoparticles, namely chitosan-phenylalanine-poly(ethylene glycol)methyl ether, was successfully synthesized in a single step conjugating reaction via CS-HOBt in water. A systematic variation of Phe and mPEG feed ratio led us to the optimal condition which used Phe 1 mol eq. and mPEG 0.3 mol eq. to CS. In addition, 1S-CS-Phe1.0-mPEG0.3 showed the %DS of Phe and mPEG for as high as ~15 and ~13, respectively, and the values are comparable with the two step (2S-CS-Phe1.0-mPEG0.3) reaction. At that time the particle size of 1S-CS-Phe1.0-mPEG0.3 were approximately 20-50 nm which was almost similar particle size of 2S-CS-Phe1.0-mPEG0.3. This work also demonstrated that the model allergen, house dust mite (HDM), entrapment and/or immobilization on CS-Phe-mPEG was under electrostatic interaction and the hydrophobic-hydrophobic van der Waals while the optimal entrapment was at pH ~ 6-7 with entrapment efficiency for ~22 %. The in vitro studies on various types of cells, fibroblast, human keratinocytes, and PBMCs, confirmed how water-based chitosan nanoparticles performed biocompatibilty without toxicity. From preclinical implementation, the HDM-entrapped CS-Phe-mPEG nanoparticle could induce the immune response from both T helper 1 and regulatory T cells. Whereas the HDM-entrapped CS-Phe-mPEG had the ability to modulate cell-mediated immune responses by reducing IFN-γ and IL-10 secretion in allergic subject, compared to that in healthy subject. The findings described here have expanded the current basic knowledge of cellular responses to HDM, which may contribute to the development of HDM-specific immunotherapy and delivery system by using this water-based chitosan nanoparticles.

3.6 Acknowledgments

One of the authors (J.J.) acknowledges the M.Sc. scholarship from Thailand Graduate Institute of Science and Technology (TGIST) under the grant no. TG-33-09-52-033M, and Ph.D. scholarship from Dusadee Pipat fund, Chulalongkorn University. The authors would like to extend their appreciation to Intergrated Innovation Academic Center (IIAC), Centenary Academic Development Project,

Ratchadapiseksompotch research grant (the grant no. RA56/060), Chulalongkorn University, Monoclonal Antibody Production Laboratory, BIOTEC, NSTDA for ELISA, the Faculty of Pharmacy, Silpakorn University for the suggestion of HPLC technique, and the Hitachi-High Technology Co., Ltd., Japan for TEM analysis. This study was supported in part by the Thailand Research Fund (TRF-MRG 5180151). The authors also would like to thank Mrs. Pungjai Mongkolpathumrat for their excellent assistant in skin prick test.

3.7 References

Aiba, S.-i. (1989) Studies on chitosan: 2. Solution stability and reactivity of partially N-acetylated chitosan derivatives in aqueous media. International Journal of Biological Macromolecules, 11(4), 249-252.

Aktaş, Y., Yemisci, M., Andrieux, K., Gürsoy, R.N., Alonso, M.J., Fernandez-Megia, E., Novoa-Carballal, R., Quiñoá, E., Riguera, R., Sargon, M.F., Çelik, H.H., Demir, A.S., Hıncal, A.A., Dalkara, T., Çapan, Y., and Couvreur, P. (2005) Development and Brain Delivery of Chitosan–PEG Nanoparticles Functionalized with the Monoclonal Antibody OX26. Bioconjugate Chemistry, 16(6), 1503-1511.

Ameal, A., Vega-Chicote, J.M., Fernandez, S., Miranda, A., Carmona, M.J., Rondon, M. C., Reina, E., and Garcia-Gonzalez, J.J. (2005) Double-blind and placebo-controlled study to assess efficacy and safety of a modified allergen extract of Dermatophagoides pteronyssinus in allergic asthma. Allergy, 60(9), 1178-1183.

Atherton, J. C. (2003) Acid-base balance: maintenance of plasma pH. Anaesthesia & Intensive Care Medicine, 4(12), 419-422.

Bal, S.M., Slütter, B., Verheul, R., Bouwstra, J.A., and Jiskoot, W. (2012) Adjuvanted, antigen loaded N-trimethyl chitosan nanoparticles for nasal and intradermal vaccination: Adjuvant- and site-dependent immunogenicity in mice. European Journal of Pharmaceutical Sciences, 45(4), 475-481.

Casettari, L., Vllasaliu, D., Mantovani, G., Howdle, S.M., Stolnik, S., and Illum, L. (2010) Effect of PEGylation on the Toxicity and Permeability Enhancement of Chitosan. Biomacromolecules, 11(11), 2854-2865.

Chew, J.L., Wolfowicz, C.B., Mao, H.-Q., Leong, K.W., and Chua, K.Y. (2003) Chitosan nanoparticles containing plasmid DNA encoding house dust mite allergen, Der p 1 for oral vaccination in mice. Vaccine, 21(21–22), 2720-2729.

Cosmi, L., Santarlasci, V., Angeli, R., Liotta, F., Maggi, L., Frosali, F., Rossi, O., Falagiani, P., Riva, G., Romagnani, S., Annunziato, F., and Maggi, E. (2006) Sublingual immunotherapy with Dermatophagoides monomeric allergoid down-regulates allergen-specific immunoglobulin E and increases both interferon-γ- and interleukin-10-production. Clinical & Experimental Allergy, 36(3), 261-272.

Couvreur, P. and Puisieux, F. (1993) Nano- and microparticles for the delivery of polypeptides and proteins. Advanced Drug Delivery Reviews, 10(2–3), 141-162.

de Britto, D. and Campana-Filho, S.P. (2004) A kinetic study on the thermal degradation of N,N,N-trimethylchitosan. Polymer Degradation and Stability, 84(2), 353-361.

England, R.J.A., Homer, J.J., Knight, L.C., and Ell, S.R. (1999) Nasal pH measurement: a reliable and repeatable parameter. Clinical Otolaryngology & Allied Sciences, 24(1), 67-68.

Fangkangwanwong, J., Akashi, M., Kida, T., and Chirachanchai, S. (2006) Chitosan-Hydroxybenzotriazole Aqueous Solution: A Novel Water-Based System for Chitosan Functionalization. Macromolecular Rapid Communications, 27(13), 1039-1046.

Fangkangwanwong, J., Akashi, M., Kida, T., and Chirachanchai, S. (2006) One-pot synthesis in aqueous system for water-soluble chitosan-graft-poly(ethylene glycol) methyl ether. Biopolymers, 82(6), 580-586.

Fernandez-Caldas, E., Iraola, V., Boquete, M., Nieto, A., and Casanovas, M. (2006) Mite immunotherapy. Current Allergy and Asthma Reports, 6(5), 413-419.

Ghaemmaghami, A.M., Robins, A., Gough, L., Sewell, H.F., and Shakib, F. (2001) Human T cell subset commitment determined by the intrinsic property of antigen: the proteolytic activity of the major mite allergen Der p 1 conditions T cells to produce more IL-4 and less IFN-γ. European Journal of Immunology, 31(4), 1211-1216.

Giudice, E.L. and Campbell, J.D. (2006) Needle-free vaccine delivery. Advanced Drug Delivery Reviews, 58(1), 68-89.

Han, D., Wang, C., Lou, W., Gu, Y., Wang, Y. and Zhang, L. (2010) Allergen-specific IL-10-secreting type I T regulatory cells, but not CD4(+)CD25(+)Foxp3(+) T cells, are decreased in peripheral blood of patients with persistent allergic rhinitis. Clinical Immunology and Immunopathology, 136(2), 292-301.

Hunter, R.J. (1981) Zeta potential in colloid science: Principles and applications. Academic Press (London and New York).

Huo, M., Zhang, Y., Zhou, J., Zou, A., and Li, J. (2011) Formation, microstructure, biodistribution and absence of toxicity of polymeric micelles formed by N-octyl-N,O-carboxymethyl chitosan. Carbohydrate Polymers, 83(4), 1959-1969.

Kennedy, R., Costain, D.J., McAlister, V.C., and Lee, T.D.G. (1996) Prevention of experimental postoperative peritoneal adhesions by N,O-carboxymethyl chitosan. Surgery, 120(5), 866-870.

Kono, K., Akiyama, H., Takahashi, T., Takagishi, T., and Harada, A. (2004) Transfection Activity of Polyamidoamine Dendrimers Having Hydrophobic Amino Acid Residues in the Periphery. Bioconjugate Chemistry, 16(1), 208-214.

Kurita, K., Ikeda, H., Yoshida, Y., Shimojoh, M., and Harata, M. (2001) Chemoselective Protection of the Amino Groups of Chitosan by Controlled Phthaloylation: Facile Preparation of a Precursor Useful for Chemical Modifications. Biomacromolecules, 3(1), 1-4.

Lei, L., Gohy, J.-F., Willet, N., Zhang, J.-X., Varshney, S., and Jérôme, R. (2003) Tuning of the Morphology of Core–Shell–Corona Micelles in Water. I. Transition from Sphere to Cylinder. Macromolecules, 37(3), 1089-1094.

Mao, B.W., Gan, L.H., Gan, Y.Y., Tam, K.C., and Tan, O.K. (2005) Controlled one-pot synthesis of pH-sensitive self-assembled diblock copolymers and their aggregation behavior. Polymer, 46(23), 10045-10055.

Mao, S., Shuai, X., Unger, F., Wittmar, M., Xie, X., and Kissel, T. (2005) Synthesis, characterization and cytotoxicity of poly(ethylene glycol)-graft-trimethyl chitosan block copolymers. Biomaterials, 26(32), 6343-6356.

Mittal, M., Siddiqui, M.R., Tran, K., Reddy, S.P., and Malik, A.B. (2014) Reactive oxygen species in inflammation and tissue injury. Antioxid Redox Signal, 20(7), 1126-1167.

Molinaro, G., Leroux, J.-C., Damas, J., and Adam, A. (2002) Biocompatibility of thermosensitive chitosan-based hydrogels: an in vivo experimental approach to injectable biomaterials. Biomaterials, 23(13), 2717-2722.

Muzzarelli, R.A.A., Ilari, P., and Petrarulo, M. (1994) Solubility and structure of N-carboxymethylchitosan. International Journal of Biological Macromolecules, 16(4), 177-180.

Slütter, B., Bal, S., Keijzer, C., Mallants, R., Hagenaars, N., Que, I., Kaijzel, E., van Eden, W., Augustijns, P., Löwik, C., Bouwstra, J., Broere, F., and Jiskoot, W. (2010) Nasal vaccination with N-trimethyl chitosan and PLGA based nanoparticles: Nanoparticle characteristics determine quality and strength of the antibody response in mice against the encapsulated antigen. Vaccine, 28(38), 6282-6291.

Slütter, B., Soema, P.C., Ding, Z., Verheul, R., Hennink, W., and Jiskoot, W. (2010) Conjugation of ovalbumin to trimethyl chitosan improves immunogenicity of the antigen. Journal of Controlled Release, 143(2), 207-214.

Taranejoo, S., Janmaleki, M., Rafienia, M., Kamali, M., and Mansouri, M. (2011) Chitosan microparticles loaded with exotoxin A subunit antigen for intranasal vaccination against Pseudomonas aeruginosa: An in vitro study. Carbohydrate Polymers, 83(4), 1854-1861.

Vila, A., Sánchez, A., Janes, K., Behrens, I., Kissel, T., Jato, J. L. V., and Alonso, M.A. J. (2004) Low molecular weight chitosan nanoparticles as new carriers for nasal vaccine delivery in mice. European Journal of Pharmaceutics and Biopharmaceutics, 57(1), 123-131.

Wang, B., He, C., Tang, C., and Yin, C. (2011) Effects of hydrophobic and hydrophilic modifications on gene delivery of amphiphilic chitosan based nanocarriers. Biomaterials, 32(20), 4630-4638.

Wang, Q.Z., Chen, X.G., Liu, N., Wang, S.X., Liu, C.S., Meng, X.H., and Liu, C.G. (2006) Protonation constants of chitosan with different molecular weight and degree of deacetylation. Carbohydrate Polymers, 65(2), 194-201.

Yoksan, R. and Akashi, M. (2009) Low molecular weight chitosan-g-l-phenylalanine: Preparation, characterization, and complex formation with DNA. Carbohydrate Polymers, 75(1), 95-103.

Yoksan, R., Akashi, M., Hiwatari, K., and Chirachanchai, S. (2003) Controlled hydrophobic/hydrophilicity of chitosan for spheres without specific processing technique. Biopolymers, 69(3), 386-390.

Yu, S., Hu, J., Pan, X., Yao, P., and Jiang, M. (2006) Stable and pH-Sensitive Nanogels Prepared by Self-Assembly of Chitosan and Ovalbumin. Langmuir, 22(6), 2754-2759.

Zhang, H.X., Du, G.H., and Zhang, J.T. (2004) Assay of mitochondrial functions by resazurin in vitro. Acta Pharmacologica Sinica, 25(3), 385-389.

Zhang, W., Shi, L., An, Y., Gao, L., Wu, K., and Ma, R. (2004) A Convenient Method of Tuning Amphiphilic Block Copolymer Micellar Morphology. Macromolecules, 37(7), 2551-2555.

Zoldners, J., Kiseleva, T., and Kaiminsh, I. (2005) Influence of ascorbic acid on the stability of chitosan solutions. Carbohydrate Polymers, 60(2), 215-218.